

Assignment

Homelab HL1

Alberto Doimo 10865196

Riccardo Iacecarino 10868500

Musical Acoustics



POLITECNICO
MILANO 1863

October 23, 2023

a) Soundboard design

The geometry definition of the 2D soundboard was inspired by an existing guitar shape. The idea was to study a non symmetrical shape to find interesting and unusual solutions. In particular the board was created by drawing multiple ellipses that are then interpolated together to form a continuous curved shape. The holes are similarly shaped and positioned in the upper part.

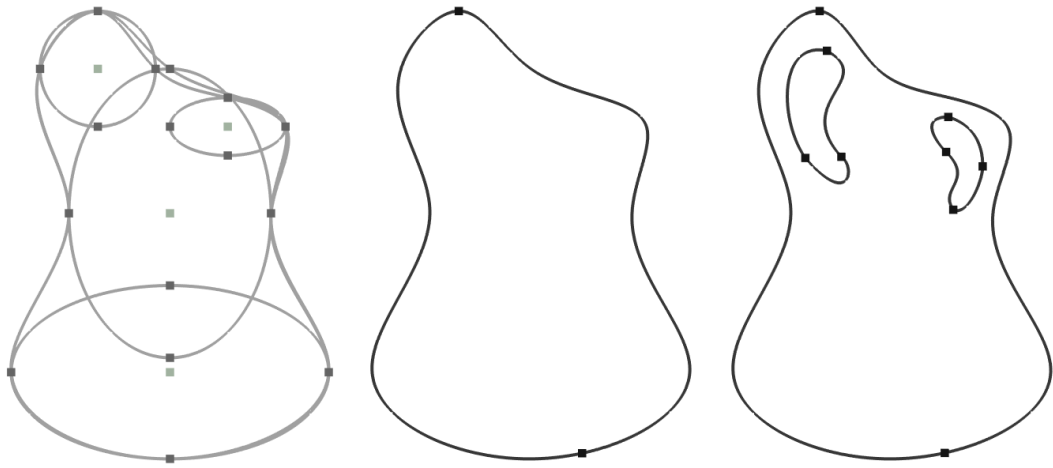


Figure 1: Design process of the soundboard

We then created the correspondent symmetric board by mirroring the previous shape w.r.t the vertical central axis, in order to analyze how differently it behaves from the original asymmetric one.

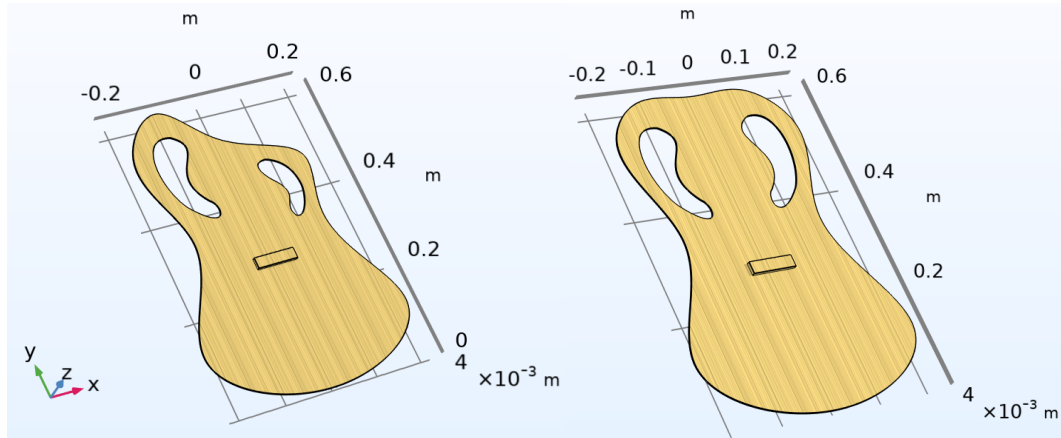


Figure 2: 3D view of the finished plates (asymmetrical and symmetrical version)

Both 2D geometries were designed in the XY Work Plane and then extruded by 2 mm along the Z-axis in order to form the 3D shape. Finally the "bridge" was formed as a rectangle of width = 85 mm and height = 22 mm, extruded by 7 mm. It has been added along the vertical central axis at a constant distance from the bottom end of both symmetric

and asymmetric boards, in order to maintain consistency between the analysis.

b) Eigenfrequency simulation: Free boundary

Once the soundboard shape was defined, in order to compute the eigenfrequencies it was necessary to apply a *material* to the geometry; in particular the chosen wood is an isotropic version of the Engelmann Spruce. To do so we defined a *blank material* with the following parameters:

- Density: $\rho = 350 \text{ [kg/m}^3\text{]}$
- Young's Modulus: $E = 9.79 \text{ [GPa]}$
- Poisson's Ratio: $\nu = 0.422$

Now, we have to introduce the *solid mechanics* physics, in order to give the software the needed physical behaviour to compute the eigenfrequencies simulation. Lastly we created a mesh for both boards. The 3D geometry was defined by a *union* of the plate and the "bridge", but keeping the interior boundaries, so that the two parts remain separated in order now to properly apply the mesh.

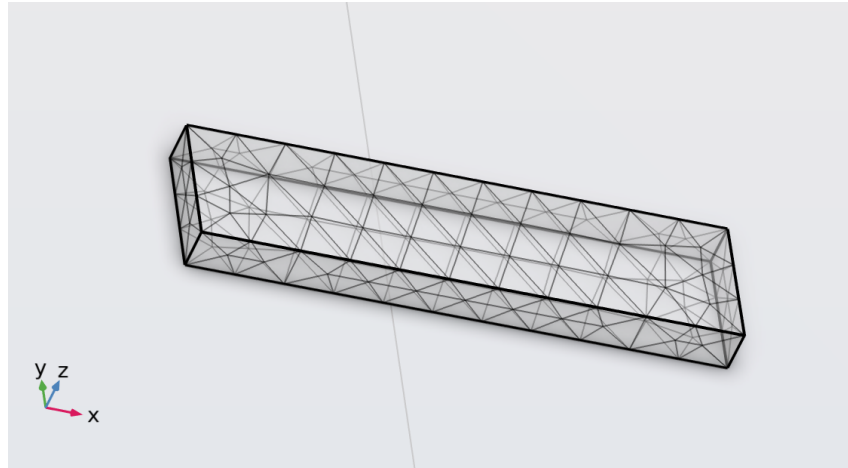


Figure 3: Close-up on the tetrahedral mesh of the bridge

Firstly we built the a *free tetrahedral* mesh over the "bridge", using the *Extra fine* size, then we defined a free triangular mesh over the surface of the plate and finally we performed a *swept* along the Z direction with *Distribution = 5* to reach the bottom part of the plate.

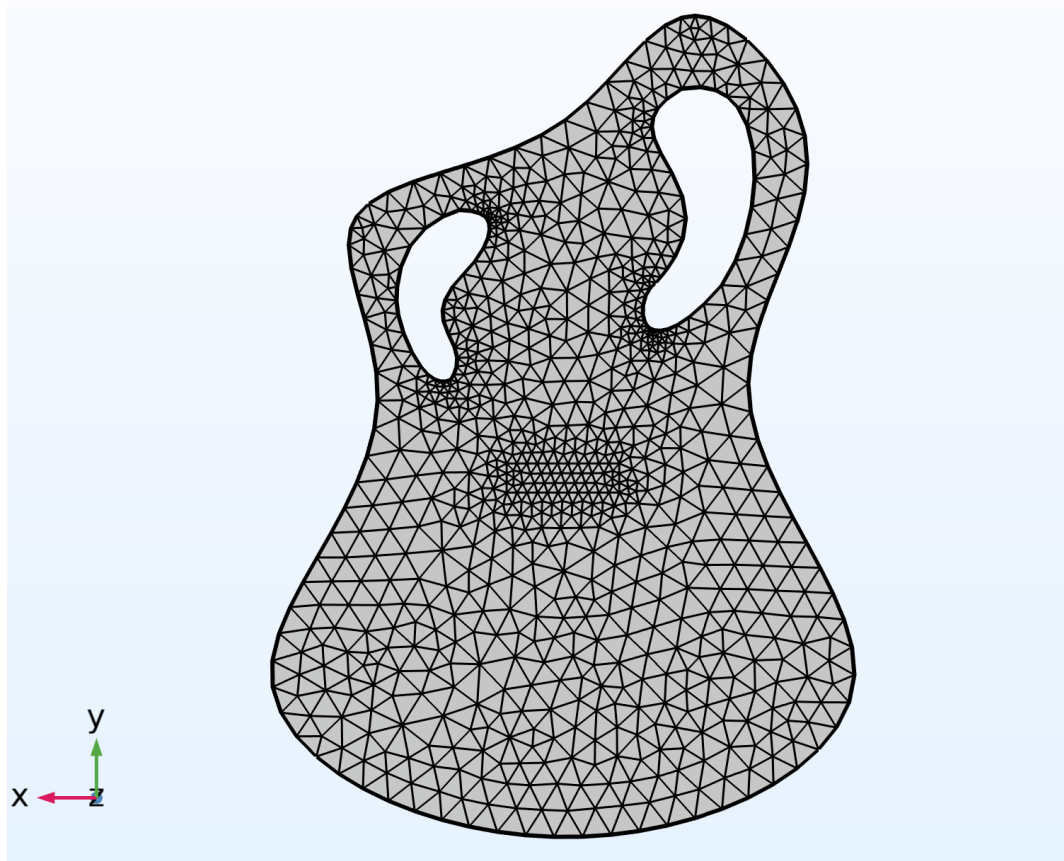


Figure 4: Rear view of the plate's mesh

The mesh was created like this in order to optimise the eigenfrequency analysis of the board: the mesh size around the "bridge", which is the most important part from the musical point of view since it transmits the vibrations from the strings to the soundboard, has been decreased by the software to make it fine and better follow the vibrational behaviour of the wood; the soundboard was modelled with a 2D triangular mesh on the surface and it was then replicated consistently through the thickness, since in this direction vibrational and physical properties remain almost constant. When these steps were completed we moved on with the actual analysis: the simulation has been done by setting the computation of 20 eigenfrequencies around 1 Hz in *free* boundary condition. The obtained results are displayed in Fig.5.

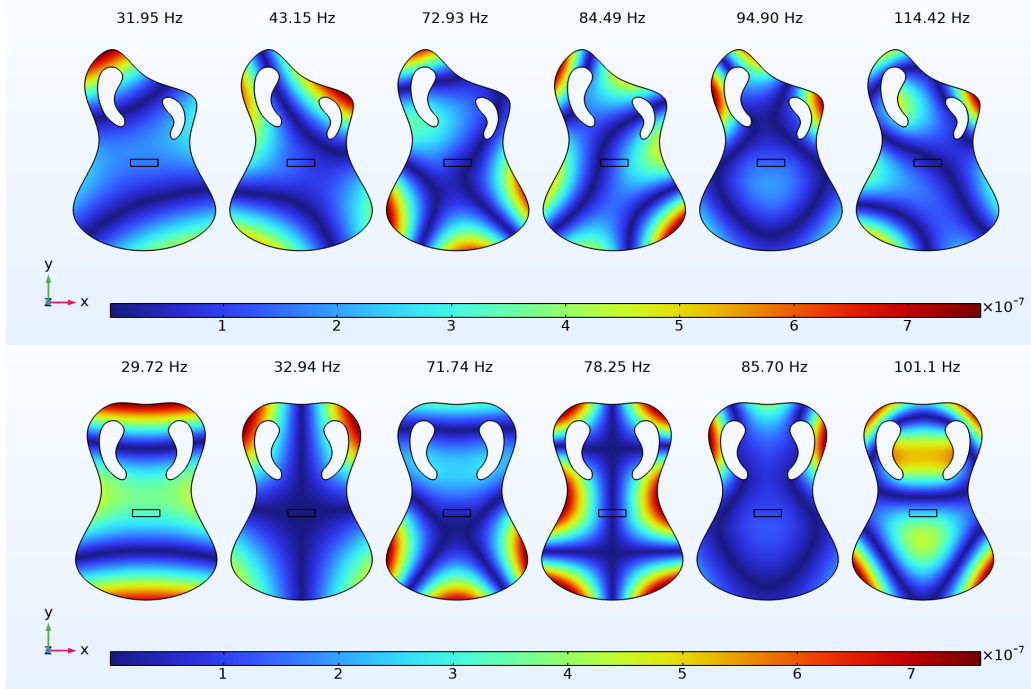


Figure 5: First six modes of free boundary vibration for asymmetrical (top) and symmetrical (bottom) soundboard of isotropic material

Looking at the soundboards we can see that correspondent modes in the two different versions of the plate differ only for a few Hz from one to the other, but the modeshape remains basically the same. A close look at them reveals that the eigenmodes are bent w.r.t the vertical axis in the asymmetric soundboard. We can notice that both geometries present only two nodal lines for the first and second frequency that progressively develop to three in the third and fourth and finally four and five in the fifth and sixth. It is interesting to notice that the non symmetric board causes a tilt of the modeshapes out of the vertical axis, to the right or the left, along an oblique one.

c) Eigenfrequency simulation: Fixed boundary

In order to compute this eigenfrequency simulation of the plate, a *fixed constraint* boundary was added to the *physics*, which was specified as the sides of the plate. The other parameters were maintained constant from the *free* boundary simulation: the material is the Isotropic Engelmann Spruce as defined in b), we are used *solid mechanics* physics and the mesh remained the same one created for the *free* case. By observing the solutions in Fig.6 we can immediately notice how the eigenfrequencies are much higher than the *free boundary* case: the first mode is shifted from 31.95 Hz to 138.19 Hz and the maxima of the displacement are never placed on the edges, contrary to what happens in the free case where they are always located on the external edges. We decided again to compare the asymmetrical soundboard with its symmetrical one, to see the differences between them and the previous case. Differently from before here it's more difficult to identify and compare similar eigenfrequencies, since they are already quite different starting from the first one and moving on to

the sixth one. However, some parallelism can still be made: the first asymmetric shape can be identified as the fundamental, since it resembles the (0,0) mode of a rectangular plate: it presents a large central displacement that progressively shades towards the edges; similarly the first mode of the symmetric shape has an internal maxima, this time shifted towards the upper part but still without nodes except from the edges. The same considerations can be made for the second eigenfrequency where again there is a similarity between the second vibrational mode of a rectangular plate and the analyzed soundboard is clearly visible, since there is a horizontal nodal line that separates the two maxima. From now on the behavior is not so clear to identify and analyze, but, comparing the symmetric and asymmetric boards in Fig.6 with the corresponding ones in the free case Fig.5 , we can say once again that the nodal lines increase in number, as the frequency goes up, and that the non symmetric board induces a shift of the modeshapes around a tilted oblique axis. It's curious finally to see how the internal parts of the curve-shaped holes frequently host one or more of the maxima of the displacement, in both the shapes considered. Intuitively, this happens because these parts are locally less constrained by the nearby material.

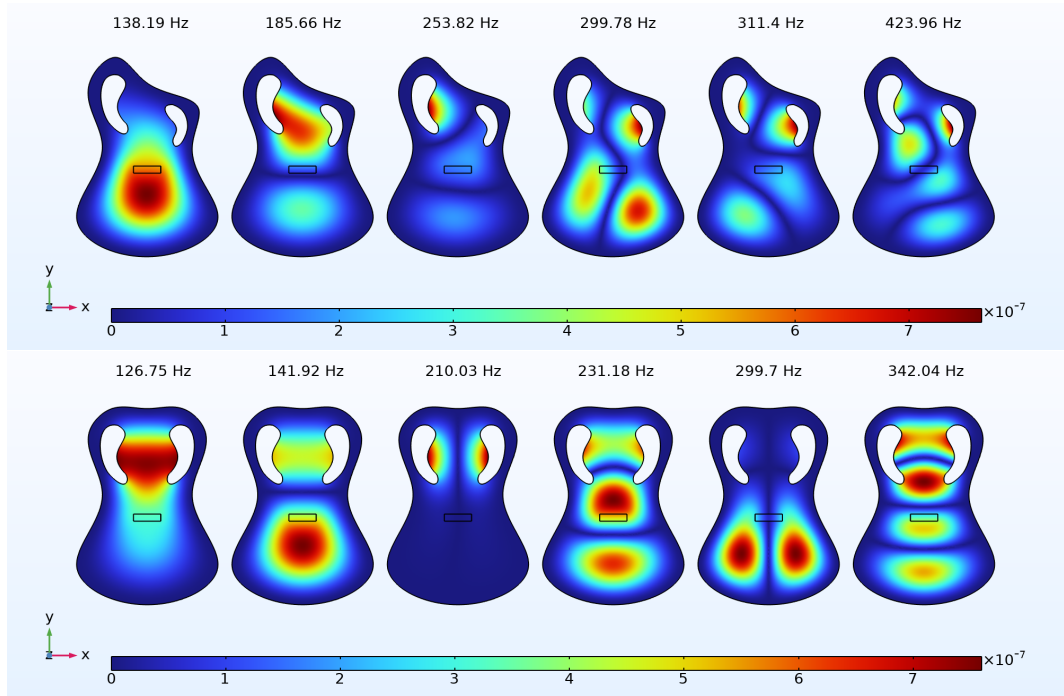


Figure 6: First six modes of fixed boundary vibration for asymmetrical (top) and symmetrical (bottom) soundboard of isotropic material

d) Eigenfrequency simulation: Orthotropic material

Referring to Tab.7 we redefined Engelmann Spruce as orthotropic, modifying the material in the dedicated section of Comsol. Moreover we had to update the *Linear Elastic Material* in the physics of the system so that it would actually consider the correct properties of the spruce.

Density [kg/m ³]			Shear Moduli [GPa]				
Engelmann Spruce	350			G_{LR}	G_{RT}	G_{LT}	
Red Maple	540		Engelmann Spruce	1.21	0.10	1.17	
Young's Moduli [GPa]			Red Maple	1.65	0.30	0.92	
	E_L	E_R	E_T	Poissons's Ratios			
Engelmann Spruce	9.79	1.25	0.58		ν_{LR}	ν_{RT}	ν_{LT}
Red Maple	12.43	1.74	0.83	Engelmann Spruce	0.422	0.53	0.462
				Red Maple	0.434	0.762	0.509

Figure 7: Table of materials' properties

For a matter of clarity, we will omit all the procedures needed to perform the free and fixed boundary studies since we have already described them previously. Furthermore, from now on we will focus our attention just on the asymmetrical soundboard, being that our main subject of study. The first analysis involves free boundary vibration and, as for the previous study, we plotted the first six modeshapes in Fig.8. Taking as a reference the asymmetrical results of Fig.5, we can derive the effects of using an orthotropic material. Above all we notice the shift in frequency towards lower values: indeed for the current study we have that the first six eigenfrequencies find themselves under 65 Hz, whereas in the same range we would find just two modes in the dual scenario. Another peculiar difference can be seen by accurately looking at the nodal lines, which now tend to settle in the direction of the fibers. The remaining observations done in point b) are still valid in broad terms for the orthotropic configuration.

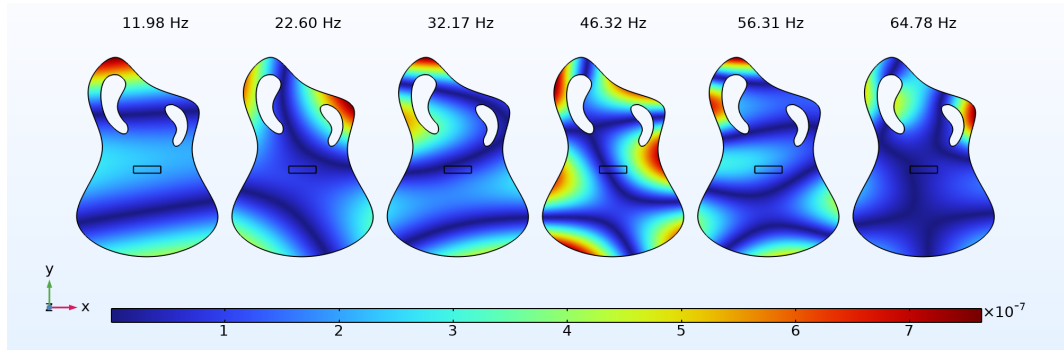


Figure 8: First six modes of free boundary vibration for the asymmetrical soundboard of orthotropic material

Coherently with the latter case, in the fixed boundary scenario we can appreciate similar transformations as regards eigenfrequencies and nodal lines in the transition from isotropic to orthotropic material. All the eigenmodes are plotted in Fig.9: despite the changes, we can also notice that not all the modes correspond to those of the isotropic case (Fig.6). A unique circumstance occurs for the third eigenfrequency, for which we can see how the bridge lays in the middle of a max.

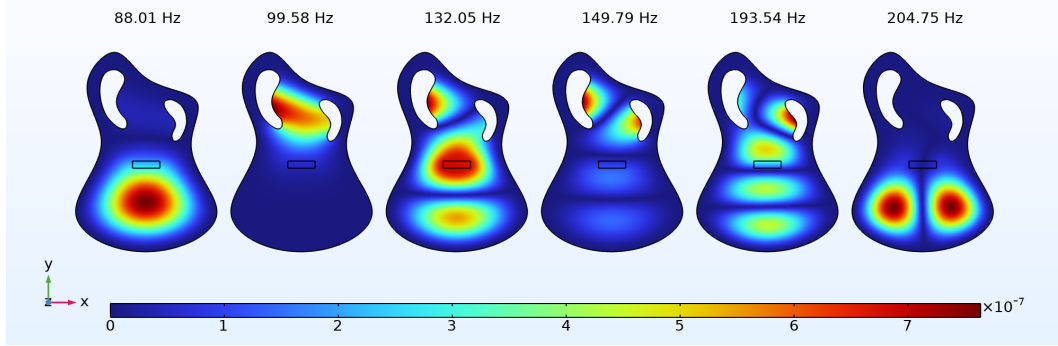


Figure 9: First six modes of fixed boundary vibration for the asymmetrical soundboard of orthotropic material

e) Loaded Maple bridge

For the next step we defined Red Maple as a new orthotropic material (see Tab.7 for its mechanical properties) that we then assigned to the bridge. Once this is done, we can exploit the *solid mechanics* section to apply a $1 [N/m^2]$ boundary load to its top surface, in the positive direction of the z-axis (perpendicular to the surface). Despite the small change, we decided to perform an additional eigenfrequency study in order to see if the introduction of the new material for the bridge returns any major difference. As expected the overall behaviour of the board didn't change, while its resonances encountered negligible alterations (1% at most) w.r.t. those indicated in Fig.8: for these reasons we decided not to plot any of this redundant information. We can now perform a *frequency domain study* of our plate on a list of regularly spaced values, with the command `range(10,0.5,70)`, thanks to which we get a set of 120 solutions linearly spaced from 10 Hz to 70 Hz. We decided to extend the range after the 6th mode of the soundboard for a matter of consistency throughout the whole report, while instead the choice of a reduced step of 0.5 Hz will be clear later in the discussion. After this list we also included the first six updated eigenfrequencies.

f) Frequency domain study results

Looking at the results of the frequency domain study (in terms of displacement) we can derive two main observations. The first thing that immediately pops out is the difference in scale reference between the first set of frequencies and the actual resonances in the system. As we can see also from the two examples reported in Fig.10, many results in the linearly spaced set are in the amplitude range of $10^{-6}, 10^{-7} [m]$, whereas when we look at the results at an eigenfrequency value the magnitude scale of the displacement increases of three orders ca.

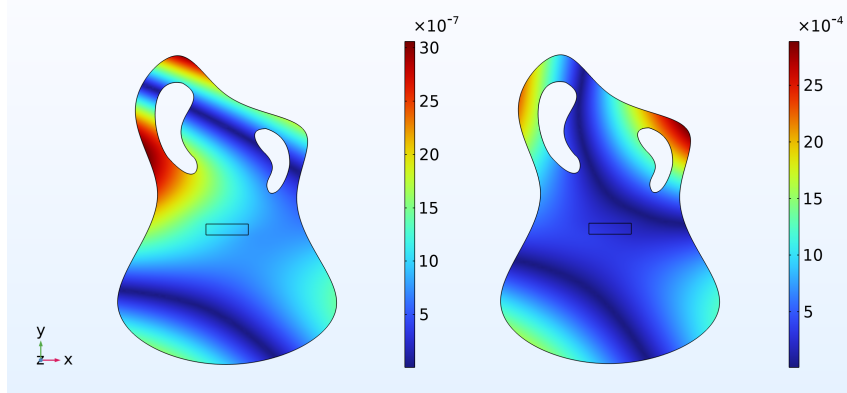


Figure 10: Left: result of the frequency study at 27.5 Hz. Right: result of the frequency study at the eigenfrequency 22.61Hz

Another meaningful comment that we can do thanks to this study is the progressive shaping of the nodal lines on the soundboard. In particular, in a first run of the study, we initially set the step to be of 2.5 Hz, but then we noticed how subsequent results were strictly related in terms of geometric shape of the displacement field (even if the scale was not the same along the 24 plots). For this reason we increased the definition up to the step of 0.5 Hz, so that the changes between a plot and the next one are slightly noticeable. To better visualize this behaviour, we exported an animated GIF file, for which we purposely deselected the COMSOL option: *synchronize scales between frames*.

g) Velocity

The final part of this analysis focuses on computing the velocity as a function of the frequency along the direction perpendicular to the plate at the bridge position. In particular, we studied the velocity field of the bridge's rear face (the contact area with the plate) by first computing its surface average in the *Derived Values* section. Doing so, we populate a table from which we can extract the data needed for the 1D plot reported in Fig.11. Once again we can appreciate the choice of the smaller step previously discussed, that in this case translates into an increased resolution of the graph.

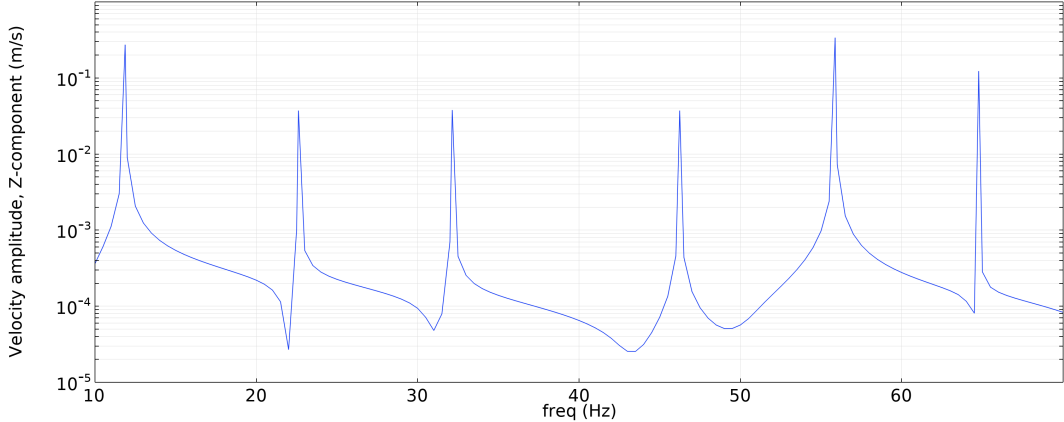


Figure 11: Average surface velocity along the Z-axis computed on the contact area between bridge and soundboard

From the plot we can immediately recognize the peaks of the first six modes (we recall that they correspond to those of Fig.8), which have different amplitudes depending on the modeshape and in which area the bridge lays. Generally speaking, if we have a mode with a nodal line that completely crosses the bridge, we can't see its associated peak in the surface velocity plot. In our case instead we can see a similar behaviour (low velocity value) in the minima of Fig.11, in which the aforementioned crossing happens but, since we are not considering any eigenfrequency we will still be able to observe every resonance included in the range. Moreover we can validate these statements by comparing two results from the *frequency domain study* of point f) (which namely presents the displacement, that follows an analogous trend). Specifically, in Fig.12 we compare the eigenfrequency with the largest velocity (55.87 Hz) to the sample with the lowest (22 Hz) and the scale alongside to the modeshape confirm our thesis.

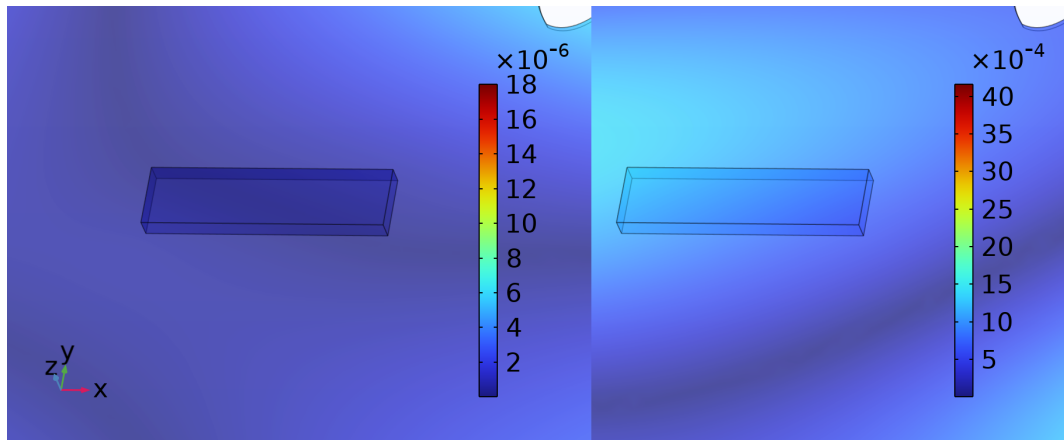


Figure 12: Close-ups of the bridge at: 22 Hz (left), 55.87 Hz (right)